This article has been accepted for publication in a future issue of this journal, but has not been fully edited. Content may change prior to final publication. Citation information: DOI 10.1109/TSG.2016.2544939, IEEE Transactions on Smart Grid

Data-Driven Pricing Strategy for Demand-Side Resource Aggregators

Zhiwei Xu, *Student Member, IEEE*, Tianhu Deng, Zechun Hu, *Member, IEEE*, Yonghua Song, *Fellow, IEEE* and Jianhui Wang, *Senior Member, IEEE*

***Abstract*—We consider a utility who seeks to coordinate the energy consumption of multiple demand-side flexible resource aggregators. For the purpose of privacy protection, the utility has no access to the detailed information of loads of resource aggregators. Instead, we assume that the utility can directly observe each aggregator's aggregate energy consumption outcomes. Furthermore, the utility can leverage resource aggregator energy consumption via time-varying electricity price profiles. Based on inverse optimization technique, we propose an estimation method for the utility to infer the energy requirement information of aggregators. Subsequently, we design a data-driven pricing scheme to help the utility achieve system-level control objectives (e.g., minimizing peak demand) by combining hybrid particle swarm optimizer with mutation (HPSOM) algorithm and an iterative algorithm. Case studies have demonstrated the effectiveness of the proposed approach against two benchmark pricing strategies – a flat-rate scheme and a time-of-use (TOU) scheme.**

***Index Terms*—Inverse optimization, data-driven optimization, demand response, dynamic pricing, particle swarm optimization(PSO)**

NOMENCLATURE

Sets/Abbreviations

$\mathcal{B}^i$	Aggregator i's uncertainty set of the right-hand side vector (b^i). See Section IV for details.
$\mathcal{I}$	Set of aggregators with index i.
$\mathcal{J}_{i,z}$	Set of type-z resource under aggregator i with index j.
$\mathcal{Z}$	Set of demand-side resource types with index z.
N	Non-deferrable loads.
V	Plug-in electric vehicles (PEV).

Parameters

β	Weight coefficient. See Section V for details.
δ	The length of a time interval, in hour.
ρ	Charging efficiency of PEV.
$a^{i,V,j}$	The arrival time step of the j-th PEV under aggregator i for charging.
b^i	The true right-hand side constraint vector of aggregator i. See Section IV for details.
$C^{i,V,j}$	The battery size of of the j-th PEV under aggregator i, in kWh.
$d^{i,V,j}$	The departure time step of the j-th PEV under aggregator i for the next trip.
$\underline{e}_t^{i,z,j}(\overline{e}_t^{i,z,j})$	The lower (upper) bound of cumulative energy consumption of resource j of type z under aggregator i at time step t, in kWh.
$\underline{E}_t^i(\overline{E}_t^i)$	The lower (upper) bound of cumulative energy consumption of aggregator i at time step t, in kWh.
$G^{i,V,j}$	The rated charging power of the j-th PEV under aggregator i. in kW.
M	A large constant.
$\underline{p}_t^{i,z,j}(\overline{p}_t^{i,z,j})$	The lower (upper) bound of power consumption of resource j of type z under aggregator i at time step t, in kW.
$\underline{P}_t^i(\overline{P}_t^i)$	The lower (upper) bound of cumulative energy consumption of aggregator i at time step t, in kW.
$s_a^{i,V,j}$	The arrival state of charge (SOC) of the j-th PEV under aggregator i.
$s_d^{i,V,j}$	The minimum departure SOC of the j-th PEV under aggregator i specified by the PEV owner.
$\overline{s}^{i,V,j}$	The upper limit of the SOC of the j-th PEV under aggregator i.
T	The length of the planning horizon.

Variables

$\hat{b}^i$	The worst-case realization of the right-hand constraint vector of aggregator i in $\mathcal{B}^i$. See Section V for details.
c_t^i	The electricity price for aggregator i at time step t, in \$/kWh.
L_p	The aggregate peak demand of utility, in kW.
$p_t^{i,z,j}$	The power consumption of resource j of type z under aggregator i at time step t, in kW.
P_t^i	The aggregate power consumption of all resources under aggregator i, in kW.
P_t^{i*}	The optimal aggregate power consumption of aggregator i, in kW.
w_t^i	Ancillary binary variable, see Section V for details.

This work was supported in part by the National Natural Science Foundation of China (51477082).

Zhiwei Xu, Zechun Hu and Yonghua Song are with the Department of Electrical Engineering, Tsinghua University, Beijing, 100084, P. R. China

Tianhu Deng is with the Department of Industrial Engineering, Tsinghua University, Beijing, 100084, P. R. China.

Jianhui Wang is with Argonne National Laboratory, Lemont, IL 60439 USA.

Corresponding author: Zechun Hu (zechhu@tsinghua.edu.cn)

I. INTRODUCTION

THE growing demand for electricity and increasing penetrations of uncertain and intermittent renewable energy present great challenges for maintaining the real-time balance between electricity production and consumption in power grids. Demand response, which aims at exploiting the inherent

flexibility on the demand side, has been regarded as an effective and efficient approach to meeting these challenges [1]. The previous work has considered various types of flexible resources at the demand side, such as plug-in electric vehicles (PEVs) [2] and thermostatically controlled loads (TCLs) [3], etc. In this paper, we consider a utility who seeks to coordinate the energy consumption of multiple demand-side flexible resource aggregators via time-varying electricity prices.

Envisaged to be the third-party participants at the demand side, aggregators are assumed to be responsible for managing the energy consumption of a group of mixed flexible loads (e.g., PEV charging demand, TCLs, etc.) and optimally respond to the time-varying electricity prices with respect to the energy requirements of their loads [4]. For this reason, pricing strategy is considered as an effective lever in coordinating the energy consumption of multiple aggreagtors, e.g., reducing aggregate peak demand. In the literature, real-time pricing models include the demand elasticity based models [5]–[7] and the adaptive pricing schemes [8], [9]. In the demand elasticity based models, the estimated self and cross-time elasticity factors are incorporated into the pricing formulation. The adaptive pricing schemes rely on the frequent two-way communications between users and utility company, which may not be desirable when deployed in large scale and communication resources are scarce.

In fact, the energy requirements of aggregators' loads is the most valuable information for the utility to fully take advantage of the pricing strategy. However, this information is generally not accessible due to privacy protection purposes. To address this challenging practical concern, we propose to apply the inverse optimization [10] technique to the estimation of the energy requirements of aggregators. In practice, though the utility has no access to exact information of energy requirements of aggregators' loads, it can infer this information by exploiting the inherent relationships between historical prices and aggregate energy consumption profiles. In the optimization terminology, inverse optimization is proposed as an effective technique to estimate the coefficients of an optimization problem via the observations of its solution. Based on the estimation results, we can further design a sophisticated pricing strategy for the utility to realize system-level control objectives.

In this paper, we first propose a compact demand-side flexible resource model to characterize the flexibility of an aggregation of heterogenous flexible resources. To generate energy consumption data of aggregators, consistent with known price data, we formulate a cost minimization model for the aggregators based on the proposed resource model, and simulate their energy consumption behavior under a number of randomly generated price profiles. Using the above generated price-consumption data, an estimation method is proposed to reveal the feasible region of the aggregator's energy consumption requirement data. We then present a data-driven pricing scheme based on the estimation results, which is autonomously responded to by the aggreagtors, to effectively help the utility achieve a lower aggregate peak demand.

To the best of our knowledge, we are the first to apply the idea of the inverse optimization to determine optimal prices in the area of demand response. Different from other pricing approaches adopted in the literature, the inverse optimization technique directly seeks to infer the information on how the aggregators determine their power consumption. In a similar vein, Ruiz et al [11] use the inverse optimization technique to reveal the marginal offer prices of a producer's rivals in the electricity market. However, their object is different from ours in that they aim to estimate the coefficients of the objective function but we work to reveal the right-hand side coefficients of the constraints.

The contributions of this paper are fourfold:

1) developing an estimation method to infer an aggregator's energy consumption requirements via historical observations of price-consumption data;
2) formulating the data-driven pricing problem as a two-stage robust optimization model;
3) proposing to combine two algorithms to iteratively solve the proposed two-stage robust model. In particular, we design an iterative algorithm to first solve the inner stage of the problem and utilize a hybrid particle swarm optimizer with mutation (HPSOM) algorithm to tackle the outer stage of the problem.
4) demonstrating the effectiveness of the proposed pricing scheme through comparisons against two other benchmark pricing schemes.

The remainder of this paper is organized as follows. The demand side flexibility model and data-driven pricing architecture are first introduced in Section II. The energy consumption optimization model of the aggregator is presented in Section III. The approach to estimating the aggregator's energy requirements is provided in Section IV. We then present the data-driven pricing model of the utility in Section V. Section VI presents the numerical simulations and the paper is concluded in Section VII.

II. Demand-side Flexibility Modeling and Data-driven Pricing Architecture

In what follows, we discretize the planning time horizon into T discrete intervals with step size δ, and assume that the power consumption of a demand-side resource is constant over each δ. We use superscript $\{i : i \in \mathcal{I}\}$ to index an aggregator, superscript $\{z : z \in \mathcal{Z}\}$ to index a set of resources that are belong to the same type (e.g., PEV etc.), superscript $\{j : j \in \mathcal{J}_{i,z}\}$ to index a type-z resource under aggregator i, and subscript $\{t : t = 1, \cdots, T\}$ to index each time interval. For example, the power consumption of the jth resource of type z under aggregator i at time step t is denoted as $p_t^{i,z,j}$. We use N and V to denote the set of non-deferrable loads and PEVs, respectively. In addition, we use P_t^i (i.e., $P_t^i = \sum_{z\in\mathcal{Z}} \sum_{j\in\mathcal{J}_{i,z}} p^{i,z,j}$) to denote the aggregate power consumption of all resources under aggregator i, where the index z and j are dropped simultaneously.

A. Demand-side Flexible Resource Modeling

We model the demand-side resources by their power and cumulative energy consumption limits over time. Specifically, we define the demand-side flexible resource model as follows.

This article has been accepted for publication in a future issue of this journal, but has not been fully edited. Content may change prior to final publication. Citation information: DOI 10.1109/TSG.2016.2544939, IEEE Transactions on Smart Grid

Definition 1. *A demand-side flexible resource is described by a series of quadruples* $(\underline{p}_t^{i,z,j}, \overline{p}_t^{i,z,j}, \underline{e}_t^{i,z,j}, \overline{e}_t^{i,z,j})$ *, where* $t: t = 1, \cdots, T$*. For each resource* j *of type* z *under aggregator* i*, the demand-side flexible resource model characterizes its lower and upper power (cumulative energy) consumption limits,* $\underline{p}_t^{i,z,j}, \overline{p}_t^{i,z,j}$ $(\underline{e}_t^{i,z,j}, \overline{e}_t^{i,z,j})$ *at time step* t*. Specifically,*

$$\underline{p}_t^{i,z,j} \leq p_t^{i,z,j} \leq \overline{p}_t^{i,z,j}, \forall t, \tag{1a}$$

$$\underline{e}_t^{i,z,j} \leq \sum_{\tau=1}^{t} p_\tau^{i,z,j} \delta \leq \overline{e}_t^{i,z,j}, \forall t. \tag{1b}$$

In what follows, we seek to derive the power and cumulative energy consumption limits for different types of demand-side flexible resources.

B. Non-deferrable Load Modeling

The non-deferrable load, which normally cannot be shifted or curtailed, is traditionally characterized by a series of fixed power consumption over time ($p_t^{i,N,j}$). In order to describe the non-deferrable load via the proposed demand-side flexible resource model in (1), we could let the upper bound and lower bounds of the power(cumulative energy) consumption of the non-deferrable load be the same. Specifically,

$$\underline{p}_t^{i,N,j} = \overline{p}_t^{i,N,j} = p_t^{i,N,j}, \forall t, \tag{2a}$$

$$\underline{e}_t^{i,N,j} = \overline{e}_t^{i,N,j} = \sum_{\tau=1}^{t} p_\tau^{i,N,j} \delta, \forall t. \tag{2b}$$

C. Plug-in Electric Vehicle Modeling

We characterize the flexibility of a PEV charging demand by following the approach adopted in [12]. Specifically, a PEV charging demand is modeled via its minimum and maximum power consumption and requirements for energy over time. The power limits of PEV $j \in \mathcal{J}_{i,V}$ under aggregator i, which arrives for charging at $a^{i,V,j}$ and departs at $d^{i,V,j}$ for the next trip, can be expressed as follows.

$$\overline{p}_t^{i,V,j} = G^{i,V,j}, \underline{p}_t^{i,V,j} = 0, \forall t \in \{a^{i,V,j}, a^{i,V,j}+1, \cdots, d^{i,V,j}\}, \tag{3a}$$

$$\overline{p}_t^{i,V,j} = \underline{p}_t^{i,V,j} = 0, \forall t \notin \{a^{i,V,j}, a^{i,V,j}+1, \cdots, d^{i,V,j}\}, \tag{3b}$$

where $G^{i,V,j}$ is its rated charging power.

The cumulative energy requirements of a PEV over time are illustrated in Fig. 1, where $\overline{s}^{i,V,j}$ is its state of charge (SOC) upper limit and $s_a^{i,V,j}$ is its SOC when it arrives for charging ($0 \leq s_a^{i,V,j} \leq \overline{s}^{i,V,j} \leq 1$). $C^{i,V,j}$ is its battery size and $s_d^{i,V,j}$ is the minimum departure SOC specified by the PEV owner. ρ is the charging efficiency.

The cumulative energy upper and lower limits ($\overline{e}_t^{i,V,j}$ and $\underline{e}_t^{i,V,j}$) of a PEV respectively correspond to its fastest and slowest path of consuming energy. In the case of upper limits, the PEV instantaneously starts charging at its rated charging power when it plugs in at $a^{i,V,j}$ until its upper limit of SOC ($\overline{s}^{i,V,j}$) is attained (from point A to point B). In the alternative case (A-D-E), the PEV's charging is first delayed (from point A to point D). Its SOC is then charged to $s_d^{i,V,j}$ at its departure

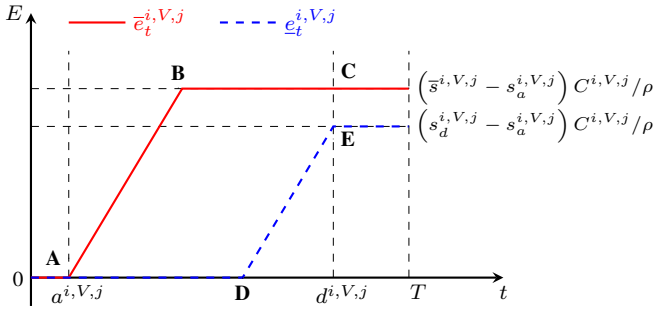

Fig. 1. Cumulative charging energy limits of a PEV.

at time $d^{i,V,j}$ (from point D to point E). The PEV owner's charging requirement is satisfied if the cumulative energy consumption at time $d^{i,V,j}$ is in between points C and E.

In previous work, it is shown that the proposed demand-side flexible resource model can be also extended to describe the flexibility characteristics of PEVs when V2G is considered, distributed energy storages and thermostatically controlled loads [13].

D. Aggregate Demand-side Flexible Resource Modeling

When we consider a set of demand-side resources of different types under aggregator i, we can first characterize each individual resource based on Definition 1. We then propose to describe the aggregate flexibility of demand-side flexible resources under this aggregator by their aggregate power and cumulative energy limits $(\underline{P}_t^i, \overline{P}_t^i, \underline{E}_t^i, \overline{E}_t^i)$, where

$$\underline{P}_t^i = \sum_{z \in \mathcal{Z}} \sum_{j \in \mathcal{J}_{z,i}} \underline{p}_t^{i,z,j}, \forall t, \tag{4a}$$

$$\overline{P}_t^i = \sum_{z \in \mathcal{Z}} \sum_{j \in \mathcal{J}_{z,i}} \overline{p}_t^{i,z,j}, \forall t, \tag{4b}$$

$$\underline{E}_t^i = \sum_{z \in \mathcal{Z}} \sum_{j \in \mathcal{J}_{z,i}} \underline{e}_t^{i,z,j}, \forall t, \tag{4c}$$

$$\overline{E}_t^i = \sum_{z \in \mathcal{Z}} \sum_{j \in \mathcal{J}_{z,i}} \overline{e}_t^{i,z,j}, \forall t. \tag{4d}$$

The advantage of this aggregate demand-side resource model is that it concisely describes the aggregate characteristics of a collection of demand side resources with only four parameters at each time step, the number of parameters used is independent of resource population size under the aggregator. Incoporating this aggregate model into the aggregator's energy consumption decision process without considering the detailed constraints and states of individual resources can efficiently facilitate the computation.

E. Data-driven Pricing and Hierarchical Coordination Architecture

In this paper, we consider a hierarchical architecture with three levels: a load level (lower level), an aggregator level (intermediate level) and the utility level (top level), see Fig. 2. We assume there is a bidirectional real-time communication infrastructure between these three levels. The utility seeks to

This article has been accepted for publication in a future issue of this journal, but has not been fully edited. Content may change prior to final publication. Citation information: DOI 10.1109/TSG.2016.2544939, IEEE Transactions on Smart Grid

coordinate the energy consumption of aggregators to achieve system-level objectives (e.g., peak shaving, revenue maximization). However, the utility is assumed to have neither the access to the detailed load information of aggregators nor the right to directly control their energy consumption for the purpose of privacy protection. Instead, it can only observe the aggregate power consumption profile of each aggregator as a response to its broadcast electricity prices. By learning the aggregator's energy consumption behavior under different price scenarios, the utility dynamically updates its beliefs on an aggregator's energy requirement constraints and formulates electricity price incentives for each aggregator.

With the broadcast electricity prices from the utility, the decision making process of each aggregator can be briefly described as follows. First, each resource under the aggregator is modeled via the flexible resource model. Second, based on the received information of flexible resource models of all loads, the aggregator constructs the aggregate flexible resource model. It is noted that though the individual flexible resource model may not be able to perfectly characterize each load due to stochastic disturbances and uncertainties, we expect the aggregate flexible resource model after pooling can reasonably describe the aggregate characteristics of the aggregator when a sufficient number of loads are gathered at the aggregator level since the variations of individual loads tend to cancel out each other. Third, based on the aggregate flexible resource model and the received price information from the utility, the aggregator makes optimal decisions on the aggregate power consumption over the planning horizon. Finally, the aggregator allocates the resulting aggregate power to individual loads based on their updated state information in real time. This paper primarily focuses on load modeling and aggregation (Section II), aggregate power consumption optimization at the aggregator level (Section III), energy requirements estimation at the utility (Section IV) and optimal pricing strategy (Section V), but does not further concern about the final power allocation step, please refer to [14] for related algorithms on scheduling.

III. Energy Consumption Optimization Model at the Aggregator Level

In this study, we assume the aggregators make the energy consumption decisions via a cost minimization model. The aggregator's optimal energy consumption profile is bounded by its power and energy limits defined in (4) by aggregating the power/energy consumption limits of individual loads. Let $P^{i,*}$ be aggregator i's optimal consumption profile, i.e., $P^{i,*}$ is the optimal solution of the following optimization model:

$$P^{i,*} \in \arg\min_{P^i \geq 0} \left\{ \sum_{t=1}^{T} c_t^i P_t^i \middle| \underline{P}_t^i \leq P_t^i \leq \overline{P}_t^i, \underline{E}_t^i \leq \sum_{\tau=1}^{t} P_\tau^i \delta \leq \overline{E}_t^i, \forall t \right\}, \tag{5}$$

where c_t^i is the electricity price for aggregator i at time step t, in \$/kWh.

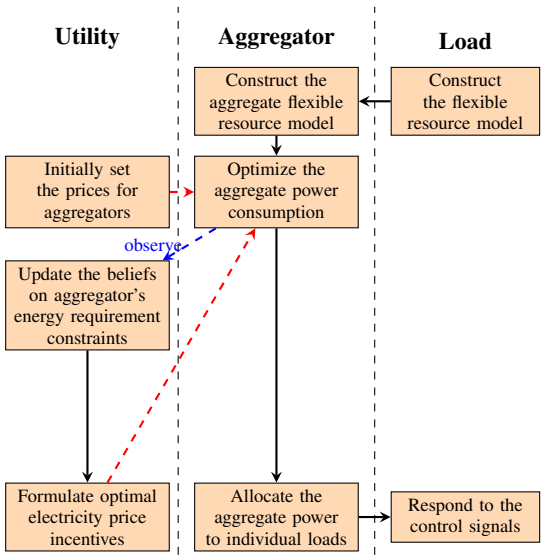

Fig. 2. Data-driven pricing and hierarchical coordination architecture.

IV. Estimating An Aggregator's Power and Cumulative Energy Consumption Boundaries

With the observations of the optimal power consumption of each aggregator $P^{i,*}$, the utility seeks to estimate the aggregator i's power and cumulative energy consumption boundaries $(\underline{P}_t^i, \overline{P}_t^i, \underline{E}_t^i, \overline{E}_t^i)$.

For expositional simplicity, we rewrite each aggregator's optimization problem as a standard form minimization problem. Aggregator i's optimization problem (5) can be equivalently rewritten in a matrix form representation:

$$\min_{P^i} \ (c^i)^T P^i \tag{6a}$$

$$\text{s.t. } A^i \cdot P^i \leq b^i, \tag{6b}$$

$$P^i \geq 0, \tag{6c}$$

where c^i is the column vector $< c_1^i, c_2^i, \ldots, c_T^i >$ and constraint $A^i \cdot P^i \leq b^i$ is a matrix form representation of

$$\underline{P}_t^i \leq P_t^i \leq \overline{P}_t^i, \underline{E}_t^i \leq \sum_{\tau=1}^{t} P_\tau^i \delta \leq \overline{E}_t^i. \tag{7}$$

Note that c^i is the price profile from the utility, P^i is the energy consumption profile determined by the aggregator and can be observed by the utility. A^i is a deterministic matrix with elements from $\{-1, 0, 1\}$, and is known to the utility. b^i, however, which contains the aggregator's information of power and cumulative energy boundaries, is generally inaccessible to the utility and is needed to be estimated based on the observable c^i and corresponding P^i.

To infer b^i, we further introduce a vector of slack variables S^i, and obtain the following equivalent standard form representation:

$$\min_{P^i, S^i} \ (c^i)^T P^i \tag{8a}$$

$$\text{s.t. } A^i \cdot P^i + S^i = b^i, \tag{8b}$$

$$P^i \geq 0, S^i \geq 0. \tag{8c}$$

This article has been accepted for publication in a future issue of this journal, but has not been fully edited. Content may change prior to final publication. Citation information: DOI 10.1109/TSG.2016.2544939, IEEE Transactions on Smart Grid

For a given b^i, denote ($P^{i*}(b^i)$,$S^{i*}(b^i)$) as the optimal primal basic feasible solution. Meanwhile, for the standard form minimization problem (8), we define $B^{i*}(b^i)$ as the basis and let $c_B^{i*}(b^i)$ be the vector of objective coefficients of the basis. By definition, $B^{i*}(b^i)$ and $c_B^{i*}(b^i)$ satisfy the feasibility condition $(B^{i*}(b^i))^{-1}b^i \geq 0$ and the optimality condition $(c_B^{i*}(b^i))^T(B^{i*}(b^i))^{-1}A \leq (c^i)^T$ and $(c_B^{i*}(b^i))^T(B^{i*}(b^i))^{-1} \leq 0$. The utility's task is to estimate the values of b^i. The following result provides an intuitive estimation.

Let $\hat{P}^i_{(1)}$, $\hat{P}^i_{(2)}$, ... and $\hat{P}^i_{(n)}$ be the observed power consumption of aggregator i when the prices are $\hat{c}^i_{(1)}$, $\hat{c}^i_{(2)}$, ..., and $\hat{c}^i_{(n)}$, respectively. Because $\hat{P}^i_{(1)}$, $\hat{P}^i_{(2)}$, ... and $\hat{P}^i_{(n)}$ are feasible power consumption, the real b^i satisfies

$$b^i \geq A^i \cdot \hat{P}^i_{(l)}, 1 \leq l \leq n. \tag{9}$$

Define $\underline{b}^i$ as the minimum possible b^i that satisfies (9). The following proposition suggests that $\underline{b}^i$ is one possible value of the real b^i.

Proposition 1. *For any* $1 \leq l \leq n$,

$$\begin{aligned}(\hat{c}^i_{(l)})^T\hat{P}^i_{(l)} = \min_{P^i}\ & (\hat{c}^i_{(l)})^T P^i \\ \textit{s.t.}\ & A^i \cdot P^i \leq \underline{b}^i, \\ & P^i \geq 0.\end{aligned} \tag{10}$$

Proof. See Appendix A. □

The following proposition specifies the range of right hand values b^i under which the optimal value $P^{i*}(b^i)$ remains constant.

Proposition 2. *Under a given* b^i *that generates the observed consumption, for any* $\hat{b} \geq b^i$ *that satisfies*

$$(B^{i*}(b^i))^{-1} \cdot \hat{b} \geq 0, \tag{11a}$$

$$(c_B^{i*}(b^i))^T \cdot (B^{i*}(b^i))^{-1} \cdot \hat{b} = (c^i)^T P^{i*}(b^i), \tag{11b}$$

we have

$$\begin{aligned}(c^i)^T P^{i*}(b^i) = \min_{P^i, S^i}\ & (c^i)^T P^i \\ \textit{s.t.}\ & A^i \cdot P^i + S^i = \hat{b}, \\ & S^i \geq 0.\end{aligned} \tag{12}$$

Proof. See Appendix B. □

Proposition 2 suggests that (11) provides the range of the right hand side values under which the optimal value and optimal solution remain constant.

In sum, Proposition 1 provides an initial estimate of real b^i. Proposition 2 allows us to construct a feasible region of the real b^i from an initial estimate of b^i. Due to Propositions 1 and 2, we are able to construct a feasible region of real b^i instead of precisely estimating the real b^i. Every feasible solution in this feasible region generates the observed consumption. In this sense, the estimation method is robust and effective theoretically. For notational convenience, we let $\mathcal{B}^i$ be the set of b^i. We infer that Propositions 1 and 2 can help us, at least partly, characterize $\mathcal{B}^i$.

V. Data-driven Pricing Strategy of the Utility

A. Mathematical Formulation

With only the estimation of the feasible region $\mathcal{B}^i$, the utility cannot predict the responses of aggregators precisely when the price profiles are generated. However, the utility still seeks to formulate the best possible pricing strategy, when being autonomously responded to by each aggregator, that can also optimize the utility level objectives (e.g., peak shaving, revenue maximization, etc.). Here, we present the following two-stage robust optimization model to optimize the pricing strategy for the utility when the worst-case realization of b^i in $\mathcal{B}^i$ occurs.

$$\text{(P1)}\quad \min_{c^i} \max_{\hat{b}^i \in \mathcal{B}^i, w, L_p} \quad L_p - \beta \cdot \sum_{i\in\mathcal{I}}\sum_{t=1}^{T} c_t^i P_t^{i*}\delta \tag{13a}$$

Subject to:

$$L_p - M \cdot w_t \leq \sum_{i\in\mathcal{I}} P_t^{i*} \leq L_p, \forall t, \tag{13b}$$

$$\sum_{t=1}^{T} w_t \leq T - 1, \tag{13c}$$

$$w_t \in \{0,1\}, \forall t, \tag{13d}$$

$$P^{i*} \in \arg\min_{P^i \geq 0} \left\{ \sum_{t=1}^{T} c_t^i P_t^i \,\middle|\, A^i \cdot P^i \leq \hat{b}^i \right\}, \forall i \in \mathcal{I}, \tag{13e}$$

$$\sum_{t=1}^{T} c_t^i = 1, \forall i \in \mathcal{I}, \tag{13f}$$

where L_p is a continuous decision variable, represented as the aggregate peak demand. M is a large constant and w_t are binary variables. c_t^i, decision variable, is the electricity price for aggregator i at time step t. P_t^{i*} are also decision variables, represented as the optimal aggregate power consumption profile of aggregator i as indicated in constraints (13e). The above model is a multi-objective optimization problem, where β is used as a weighting factor (in kW/$) to help the utility make tradeoffs between the two objectives. Specifically, the utility has two control objectives. In (P1), the first term of the objective function is to minimize the aggregate peak demand over the planning horizon. The second term maximizes the total revenue of the utility collected from aggreagtors. Constraints (13b)-(13d) ensure that there are at least one w_t that is equal to 0 and L_p is equal to the maximum aggregate demand over the planning horizon. Since individual aggregators make the optimal decisions based on the price of an interval relevant to the prices of other intervals, we introduce the normalization constraints (13f).

Note that the above formulation is a min-max two-stage problem, which cannot be directly solved by commercial softwares, such as CPLEX. Therefore, we develop an algorithm to solve the problem. In what follows, with given price c_t^i, we first develop an iterative algorithm to solve the inner stage maximization problem. We next employ a hybrid particle swarm optimizer with mutation (HPSOM) algorithm to update the values of c_t^i at the outer stage to finally solve the problem (P1).

This article has been accepted for publication in a future issue of this journal, but has not been fully edited. Content may change prior to final publication. Citation information: DOI 10.1109/TSG.2016.2544939, IEEE Transactions on Smart Grid

B. Solution Methodology for the Inner Stage of Problem (P1)

The key difficulty to solve the inner stage of (P1) lies in linearizing (13e). Since the optimization problem in (13e) is a linear program, the strong duality theorem holds. Thus, one possible linearization approach for (13e) is to first use the KKT conditions and then linearize the complementary slackness equations by introducing additional binary decision variables. But this approach introduces a large number of integer decision variables, which would make the problem computationally challenging. To facilitate the computation, we propose an iterative algorithm to solve the inner stage maximization problem of (P1) with given c_t^i.

We first equivalently transform inner stage maximization problem of (P1) to the following optimization problem:

$$\text{(P2)}\quad \mathcal{Q}(c) = \max_{\hat{b}^i, P^{i,0}, w, L_p} \; L_p - \beta \cdot \sum_{i\in\mathcal{I}} \sum_{t=1}^{T} c_t^i P_t^{i,0} \delta \tag{14a}$$

Subject to:

$$(13b) - (13d) \tag{14b}$$

$$A^i \cdot P^{i,0} \le \hat{b}^i, \forall i \in \mathcal{I}, \tag{14c}$$

$$c^T P^{i,0} \le \min_{P^i \ge 0} \left\{ \sum_{t=1}^{T} c_t^i P_t^i \,\middle|\, A^i \cdot P^i \le \hat{b}^i \right\}, \forall i \in \mathcal{I}, \tag{14d}$$

where $P^{i,0}$ is a set of newly introduced decision variables. Because $P^{i,0}$ satisfies (14c), the inequality (14d) is only valid when the $P_t^{i,0}$ is equal to the optimal solution P_t^{i*}. Therefore the equivalence between (P2) and the inner stage of problem (P1) is straightforward. To solve the reformulated (P2), we apply the following Algorithm 1.

C. Solution Methodology for (P1)

A hybrid particle swarm optimizer with mutation (HPSOM) is employed to update the values of c_t^i at the outer stage of (P1). Particle swarm optimization (PSO) is a swarm intelligent algorithm. Each particle in the swarm represents a feasible price profile c_t^i to (P1). At each iteration, the particles dynamically adjust their velocities and locations in the seaching space based on their own past experience as well as the group's experience. To avoid premature convergence of the PSO algorithm, the HPSOM algorithm incorporates the mutation process in the genetic algorithm into the original PSO algorithm. The details of this algorithm can be found in Algorithm 2 (cf. [15] [16]).

Algorithm 1: Iterative algorithm for solving (P2)

- Set the ub_i (Upper Bound) at $+\infty$ for the optimal value of aggregator i.
- Set LB (Lower Bound) at $-\infty$, UB (Upper Bound) at $+\infty$.

while *true* do

Solve the optimization problem:

$$\max_{\hat{b}^i, P^{i,0}, w, L_p} \; L_p - \beta \cdot \sum_{i\in\mathcal{I}} \sum_{t=1}^{T} c_t^i P_t^{i,0} \delta$$
$$\text{s.t. } (14b) - (14c),$$
$$(c^i)^T P^{i,0} \le ub_i, \forall i \in \mathcal{I},$$

and the optimal $\hat{b}^i$ and $P^{i,0}$ is respectively denoted as $\hat{b}^{i,*}$ and $P^{i,0,*}$ for each aggregator i and the optimal value is referred to as O^*.

Update the upper bound on $\mathcal{Q}(c)$:

$$\text{UB} \leftarrow \min\{\text{UB}, O^*\}.$$

For each aggregator i, solve the cost minimization problem:

$$\min_{P^i} \; \sum_{t=1}^{T} c_t^i P_t^i$$
$$\text{s.t. } A^i \cdot P^i \le \hat{b}^{i,*},$$
$$P^i \ge 0,$$

and the optimal solution and the optimal value is denoted as $P^{i,*}$ and $o^{i,*}$, respectively.

if $(c^i)^T P^{i,0,*} = o^{i,*}$ *for all aggregators* **then**

$\mathcal{Q}(c) = \text{UB}$

break

else

Update the upper bound for the optimal value of each aggregator i

$$ub_i \leftarrow \min\left\{ub_i, o^{i,*}\right\}.$$

end

Update the lower bound on $Q(c)$

$$\text{LB} \leftarrow \max\left\{\text{LB}, \max_{1\le t\le T} \sum_{i\in\mathcal{I}} P_t^{i,*} - \beta \cdot \sum_{i\in\mathcal{I}} \sum_{t=1}^{T} c_t^i P_t^{i,*} \delta\right\}.$$

if *UB* $-$ *LB* $\le \epsilon$ **then**

$\mathcal{Q}(c) = \text{LB}$

break

end

end

VI. Case Studies

A. Parameter Settings

For illustrative purposes, we only account for non-deferrable loads and PEV charging loads. We consider a utility and four aggregators. The first three aggregators, who are connected with both non-deferrable load and PEV charging load, are located in the residential areas. The last aggregator merely aggregates multiple rechargeable spots in a public parking deck in the vicinity of a commercial building. The non-deferrable load profiles are from an appliance energy consumption database collected near Austin, Texas in the summer of 2012. According to the empirical study on PEV charging behaviors [17], we assume the initial SOCs of the arrival private PEVs at all places follow the Gaussian distribution $\mathcal{N}(0.6, (0.1)^2)$. For residential areas, we assume the number of PEVs arriving at these three aggregators are 300, 400 and 500, respectively. Both of their arrival and departure times are assumed to be Gaussian, set as $\mathcal{N}(19{:}00, (2\text{hr})^2)$ and $\mathcal{N}(7{:}45, (1.5\text{hr})^2)$, respectively. Similarly, we assume that there are 500 PEVs arriving at the commercial places daily, and that their arrival times follow $\mathcal{N}(9{:}00, (1.5\text{hr})^2)$ and their departure times follow $\mathcal{N}(17{:}00, (0.5\text{hr})^2)$. The 1200 PEVs considered in our study are assumed to be all Tesla Model S with a 85kWh battery pack and a 10kW charger [18]. The charging efficiency ρ is 0.92 and the required departure SOCs of PEVs are all set as 1 for simplicity.

This article has been accepted for publication in a future issue of this journal, but has not been fully edited. Content may change prior to final publication. Citation information: DOI 10.1109/TSG.2016.2544939, IEEE Transactions on Smart Grid

Algorithm 2: HPSOM algorithm for solving problem (P1)
- Set the population size U, the initial inertia weight ω and the mutation probability p_m.
- Set the maximum number of iterations $maxIter$ and $k \leftarrow 0$.
- Randomly initialize U particles with the normalized random positions, $c^u = [c^{u,1}; c^{u,2}; \cdots ; c^{u,|\mathcal{I}|}]$ and their velocities $v^u = [v^{u,1}; v^{u,2}; \cdots ; v^{u,|\mathcal{I}|}]$ on $T \times |\mathcal{I}|$ dimensions in the search space.
while $k < maxIter$ **do**
- For each particle c^u, apply Algorithm 1 to evaluate the fitness value, O^u.
- Compare particle's fitness value with its $pbest^u$. If current fitness is smaller than $pbest^u$, set $pbest^u$ equal to O^u, and d^u equal to c^u.
- Find the particle in the swarm with the smallest fitness value so far $gbest$ and let $g = \arg\min_{1 \le u \le U} O^u$.
- Update the velocity and position of each particle according to the following equations:

$$v^u \leftarrow \omega \cdot v^u + \lambda^u \otimes (d^u - c^u) + \mu^u \otimes (c^g - c^u)$$
$$c^u \leftarrow \max(\psi, c^u + v^u)$$

- (**Mutation**) Generate a random number, r^u, for each particle, if $r^u < p_m$, update the particle's position by following equations:

$$\begin{cases} c^u \leftarrow \max(\psi, c^u + 0.1 \times \varphi^u), \text{ if } w^u > 0.5 \\ c^u \leftarrow \max(\psi, c^u - 0.1 \times \varphi^u), \text{ if } w^u \le 0.5 \end{cases}$$

- Normalize the upated price c^u for every aggregator of each particle
- $k \leftarrow k + 1$ and update ω
end
Use the particle c^{u*} with the least $pbest^u$ as the solution to problem (P2).
Notes*:
- λ^u, μ^u, φ^u are all vectors of randomly generated numbers uniformly distributed with support [0,1] for each particle u and are updated at each iteration.
- r^u and w^u follow uniform distribution between 0 and 1 for each particle u and are updated at each iteration.
- ψ is a sufficiently small positive constant.
- $\otimes$ represents the component-wise multiplication.
- ω is originally set as a relatively high value (e.g., 0.9) and gradually reduces to a much lower value (e.g., 0.4) with the increasing number of iterations [15].

The length of an interval δ is 15 minutes and the planning horizon is set as a day. We randomly generate 50 samples of normalized price profiles for each aggregator and collect their corresponding optimal energy consumption profiles by solving (5). Other parameters are taken as follows: $\beta = 192$ kW/$ in (13a); $\epsilon = 0.01$ in Algorithm 1; $U = 50$, $maxIter = 50$, $p_m = 0.2$ and ω is initially set as 0.9 and linearly reduces to 0.4 when the number of iterations reaches 50 in Algorithm 2. All numerical simulations are implemented using CPLEX 12.1 on Matlab platform with Core i7 2.9 GHz and 64GB memory.

B. Benchmark Pricing Strategies

In order to demonstrate the effectiveness of the proposed data-driven pricing scheme, we consider two benchmarks.

1) *Flat rate pricing scheme:* under this pricing scheme, the aggregator has no incentives to minimize its electricity costs through energy arbitrage. Instead, any PEV under this pricing scheme will start charging at its rated charging power until its battery is fully charged or its departure for next trip.

2) *Static time-of-use (TOU) pricing scheme:* this pricing scheme is widely adopted in the industry to encourage consumers to shift their energy consumption to off-peak periods and thus help reduce the system's peak demand. However, the occurrence of unexpected simultaneous consumption shifting might occur, resulting in an undesirable peak demand during the off-peak periods [19]. For simulations under this type of pricing scheme, we choose to use a normalized TOU tariff profile adopted in Shenzhen China, which is specially designed to encourage PEV off-peak charging. The off-peak and on-peak periods are set as 23:00-7:00 (next morning) and 7:00-23:00, respectively and the unit electricity price ($/kWh) during the on-peak hours are as high as four times of it during the off-peak periods.

C. Numerical Results

We simulate 24-hour energy consumption behaviors of the four aggregators starting from 12:00 pm. Fig. 3 and Fig. 4 respectively show the power consumption profiles of the four aggregators and the aggregate power consumption profile of the utility, under different pricing schemes. The optimized data-driven electricity price profiles for each aggregator are also demonstrated in Fig. 3 by the dotted blue curve.

Fig. 3 shows that, under the time-varying prices, including the proposed data-driven pricing scheme and the TOU pricing scheme, the aggregators choose to increase their power consumption (e.g., charge PEV) during the periods with lower prices. For example, when the TOU price becomes cheaper at 23:00 in the evening, the first three aggregators simultaneously start charging their connected PEVs immediately until all PEVs are fully charged around 3:00 in the morning. Under the same lower prices from 23:00 to 7:00 in the next morning, the aggregators perfer to charge their PEVs as early as possible, so as to avoid unexpected early departures. However, as the coordination between aggregators is not available when the TOU pricing is adopted, the overlapping of charging peaks at 23:00 undersirably creates another power consumption peak, as shown in Fig. 4.

Compared with the TOU scheme, the price profiles generated via the proposed data-driven approach are different across aggregators. The power consumption profiles of aggregators are negatively correlated with their electricity price profiles over time, as a result of electricity cost minimziation incentives. But it is observed that the charging peaks of different aggregators are shifted. This effectively reduces the aggregate peak demand as demonstrated in Fig. 4. Moreover, to explain why the data-driven price profiles fluctuate so much, we note that the objective of the proposed data-driven pricing strategy (P1) only considers the aggreate peak demand and the total electricity revenue for the utility, but neglects power oscillation. The oscillated power does not affect the PEV owner's comfort. The reason is that the resulting power profile strictly satisfies the power and energy consumption requirements of the aggregators, indicating that the required SOCs of the PEVs can be satisfied upon their departures.

This article has been accepted for publication in a future issue of this journal, but has not been fully edited. Content may change prior to final publication. Citation information: DOI 10.1109/TSG.2016.2544939, IEEE Transactions on Smart Grid

However, these oscillations might result in frequent switches of charging equipments. The increased switches might cause additional mechanical wear on equipment and battery degradation. Explicitly considering the switching costs in the optimization model would be helpful for the aggregator to make better tradeoffs between energy arbitrage and switching costs. However, it is not straightforward to include this cost in the formulation since we only optimize the aggregate power for all loads at each step. But this aggregate power does not uniquely determine the number of switches. To ensure the external control of PEVs is cost-efficient, a thorough cost and benefit analysis would be necessary.

The value of the data-driven pricing strategy is also verified by the inferior performance that the flat rate scheme presents in Figs. 3 and 4. With no incentives to shift the charging power of PEVs to periods of lower prices under the flat pricing scheme, the charging of PEVs is started instantaneously when they are plugged in and this undersirably overlaps with the current non-deferrable load peak, further resulting in higher peak-valley difference.

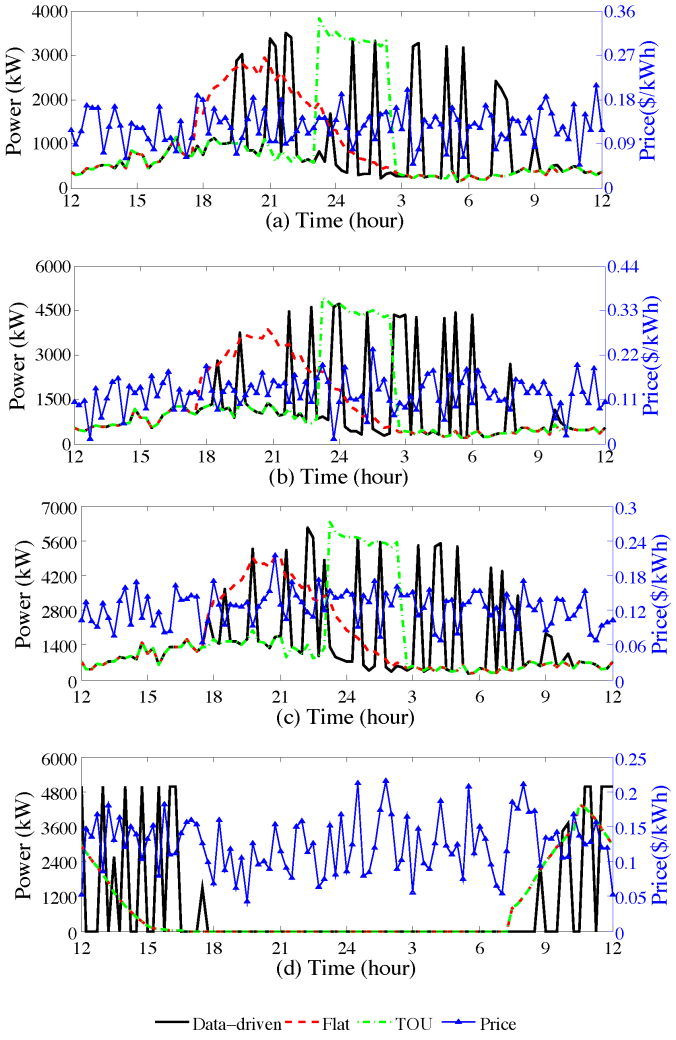

Fig. 3. Power consumption profiles of aggregators under data-driven pricing, flat pricing and TOU pricing strategies and data-driven price profile, (a)-(d) correspond to aggregators 1-4, respectively

We summarize the overall system performance under different pricing schemes in Table I. As shown in Table I, the TOU pricing strategy reduces the revenue for the utility by 14.0% as compared to the case of the flat rate scheme, due to the energy arbitrage behaviors of aggregators. However, it unexpectedly increases the aggregate peak demand by 27.9%, indicating the performance under the TOU pricing scheme might even be inferior to the simple flat rate scheme when aggregators shift their load together. The data-driven pricing scheme is shown to have the best performance in terms of alleviating aggregate peak demand, realizing a 18.1% of reduction in peak demand as compared to the flat rate scheme. But it lowers the revenue for the utility because of the aggregators' energy arbitrage. The reduced peak demand can potentially save the costs of the utility for distribution network reinforcement, which can in part compensate for the revenue loss. The utility can achieve different levels of revenue and peak demand by flexibly determining the value of β in (13a). A thorough cost and benefit analysis would be necessary to determine a proper choice of β, ensuring the resulting pricing strategy is cost-efficient.

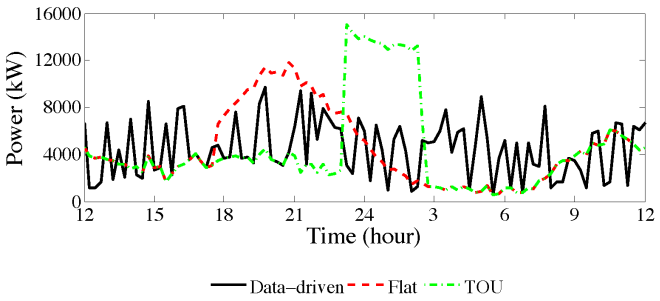

Fig. 4. Aggregate power consumption profile of the utility under data-driven pricing, flat rate pricing and TOU pricing strategies

TABLE I
OVERALL SYSTEM PERFORMANCE UNDER DIFFERENT PRICING STRATEGIES

Pricing Scheme	Total Electricity Costs*($\$/day$)	Aggregate Peak Demand (kW)	PAR**
Data-driven	962.3	9666.9	2.176
Flat	1110.8	12940.5	2.913
TOU	955.0	15084.0	3.395

*: the total electricity costs are calculated under the normalized price profiles as specified by Eqn. (13f).
**: PAR stands for peak-to-average ratio.

We next evaluate the computational efficiency of the proposed data-driven pricing strategy. Notice that both algorithms in solving the inner and outer stages of the problem involve iterations and the number of iterations at the outer stage is jointly determined by the number of particles and the maximum number of iterations, we only list the mean/maximum/minimum evaluation times that are required for solving the inner stage problem in Table II. It is observed that the computation time needed to solve the inner stage problem is not trivial. This is because the Algorithm 1 has to solve a mixed integer linear program in each iteration. To accelerate to computation, we can implement the evaluation process for each particle at the outer stage in parallel. In

This article has been accepted for publication in a future issue of this journal, but has not been fully edited. Content may change prior to final publication. Citation information: DOI 10.1109/TSG.2016.2544939, IEEE Transactions on Smart Grid

addition, considering that our pricing scheme is normally computed in day-ahead, the current computational performance is acceptable. The design of a more efficient algorithm to solve (P1) is left for future work.

TABLE II
EVALUATION TIMES FOR MAKING DECISIONS AT THE INNER STAGE

Mean (sec)	Maximum (sec)	Minimum (sec)
108.6	189.1	28.2

VII. CONCLUSIONS

This paper has explored a data-driven pricing strategy for the utility, who seeks to coordinate the energy consumption of multiple demand-side aggreagtors with flexible loads, but does not have access to the detailed information of their load requirements. Assuming that aggregators minimize their electricity costs, we first presented an estimation method for the utility to infer the power and energy boundaries of the aggregators via the observed historical price and energy consumption data. Based on the estimation results, a data-driven pricing scheme was then proposed to realize peak shaving for the utility.

Through comparisons with two benchmark pricing schemes, we found that the proposed data-driven pricing scheme can effectively realize peak demand reduction by encouraging the aggregators to shift their power consumption to different time periods. Considering that the encouragement of load shifting might degrade the revenue for the utility, in practice, the utility would need to carry out detailed cost and benefit analyses to determine a proper weighting coefficient for revenue in its control objective to make sure the generated pricing strategy is cost-efficient.

For future work, it is interesting to consider the incentive design problem where the utility functions of the aggregators are also unknown to the utility. The design of a more efficient algorithm to solve (P1) is also worthwhile for further investigations. In addition, explicit incorporation of switching costs could also limit the negative impacts of external control on PEV charging equipment and batteries that could possibly arise from power oscillations. Finally, the design of an effective mechanism to ensure the generated price profiles are fair for all aggregators may also be necessary for real implementation of the proposed pricing scheme.

APPENDIX

A. Proof of Proposition 1

Proof. First, because $\hat{P}^i_{(l)}$ is a feasible solution to

$$\min_{P^i} \ (\hat{c}^i_{(l)})^T P^i \tag{15a}$$
$$\text{s.t. } A^i \cdot P^i \le \underline{b}^i, \tag{15b}$$
$$P^i \ge 0, \tag{15c}$$

we have that

$$\begin{aligned}(\hat{c}^i_{(l)})^T \hat{P}^i_{(l)} &\ge \min_{P^i} \ (\hat{c}^i_{(l)})^T P^i \\ &\quad \text{s.t. } A^i \cdot P^i \le \underline{b}^i, \\ &\quad\quad P^i \ge 0.\end{aligned} \tag{16}$$

Further, because the real b^i must be no less than $\underline{b}^i$,

$$\begin{aligned}(\hat{c}^i_{(l)})^T \hat{P}^i_{(l)} &\ge \min_{P^i} \ (\hat{c}^i_{(l)})^T P^i \\ &\quad \text{s.t. } A^i \cdot P^i \le \underline{b}^i, \\ &\quad\quad P^i \ge 0 \\ &\ge \min_{P^i} \ (\hat{c}^i_{(l)})^T P^i \\ &\quad \text{s.t. } A^i \cdot P^i \le b^i, \\ &\quad\quad P^i \ge 0, \\ &= (\hat{c}^i_{(l)})^T \hat{P}^i_{(l)}.\end{aligned} \tag{17}$$

We infer that all the inequalities must hold at equality. □

B. Proof of Proposition 2

Proof. For this standard form minimization problem, we denote y^i as the vector of its dual variables. The dual optimization problem is

$$\max_{y^i} \ (b^i)^T y^i \tag{18a}$$
$$\text{s.t. } A^T \cdot y^i \le c^i, \tag{18b}$$
$$y^i \le 0. \tag{18c}$$

Consider a primal solution

$$(P^{i*}(b^i), S^i = \hat{b} - A^i \cdot P^{i*}(b^i))$$

and dual solution

$$(c^i_B(b^i))^T \cdot (B^{i*}(b^i))^{-1}.$$

First, the primal solution is primal feasible. The construction of S^i automatically satisfies the constraint

$$A^i \cdot P^i + S^i = \hat{b}. \tag{19}$$

Further,

$$S^i = \hat{b} - A^i \cdot P^{i*}(b^i)) \ge b^i - A^i \cdot P^{i*}(b^i)) = S^{i*}(b^i) \ge 0. \tag{20}$$

Second, the dual solution is dual feasible. Recall that the definitions of $B^{i*}(b^i)$ and $c^i_B(b^i)$ require that

$$(B^{i*})^{-1} b^i \ge 0 \tag{21}$$

and

$$(c^i_B)^T (B^{i*})^{-1} A^i \le c^T, (c^i_B)^T (B^{i*})^{-1} \le 0. \tag{22}$$

Therefore, the dual feasibility holds. Finally, the duality gap equals zero because

$$(c^i)^T P^{i*}(b^i) = (c^i_B(b^i))^T \cdot (B^{i*}(b^i))^{-1} \cdot \hat{b}. \tag{23}$$

By the strong duality theorem, the primal solution and dual solution are primal optimal and dual optimal, respectively. We infer that when (11) is satisfied, the optimal value remains to be $(c^i)^T P^{i*}(b^i)$. □

REFERENCES

[1] D. Callaway and I. Hiskens, "Achieving controllability of electric loads," *Proceedings of the IEEE*, vol. 99, no. 1, pp. 184–199, 2011.

[2] Z. Xu, W. Su, Z. Hu, Y. Song, and H. Zhang, "A hierarchical framework for coordinated charging of plug-in electric vehicles in china," *IEEE Trans. Smart Grid*, vol. pp, no. 99, 2015.

[3] J. Mathieu, S. Koch, and D. Callaway, "State estimation and control of electric loads to manage real-time energy imbalance," *IEEE Trans. Power Syst.*, vol. 28, no. 1, pp. 430–440, Feb 2013.

[4] J. L. Mathieu, M. Kamgarpour, J. Lygeros, G. Andersson, and D. S. Callaway, "Arbitraging intraday wholesale energy market prices with aggregations of thermostatic loads," *IEEE Trans. Power Syst.*, vol. 30, no. 2, pp. 763–772, 2015.

[5] D. Kirschen, G. Strbac, P. Cumperayot, and D. de Paiva Mendes, "Factoring the elasticity of demand in electricity prices," *IEEE Trans. Power Syst.*, vol. 15, no. 2, pp. 612–617, May 2000.

[6] A. K. David and Y. C. Lee, "Effect of inter-temporal factors on the real time pricing of electricity," *IEEE Trans. Power Syst.*, vol. 8, no. 1, pp. 44–52, Feb. 1993.

[7] R. Yu, W. Yang, and S. Rahardja, "A statistical demand-price model with its application in optimal real-time price," *IEEE Trans. Smart Grid*, vol. 3, no. 4, pp. 1734–1742, Dec. 2012.

[8] L. Qian, Y. A. Zhang, J. Huang, and Y. Wu, "Demand response management via real-time electricity price control," *IEEE J. Sel. Area Comm.*, vol. 31, no. 7, pp. 1268–1280, Jul. 2013.

[9] P. Samadi, A.-H. Mohsenian-Rad, R. Schober, V. W. Wong, and J. Jatskevich, "Optimal real-time pricing algorithm based on utility maximization for smart grid," in *Proc. IEEE Int. Conf. on Smart Grid Comm.*, 2010, pp. 415–420.

[10] R. K. Ahuja and J. B. Orlin, "Inverse optimization," *Oper. Res.*, vol. 49, no. 5, pp. 771–783, Sept.- Oct. 2001.

[11] C. Ruiz, A. J. Conejo, and D. J. Bertsimas, "Revealing rival marginal offer prices via inverse optimization," *IEEE Trans. Power Syst.*, vol. 28, no. 3, pp. 3056–3064, Aug 2013.

[12] O. Sundstrom and C. Binding, "Flexible charging optimization of electric vehicles considering distribution grid constraints," *IEEE Trans. Smart Grid*, vol. 3, no. 1, pp. 26–37, Mar 2012.

[13] Z. Xu, D. S. Callaway, Z. Hu, and Y. Song, "Hierarchical coordination of generalized flexible loads," *IEEE Trans. Power Syst.*, in Press 2015.

[14] C. Chen, J. Wang, and S. Kishore, "A distributed direct load control approach for large-scale residential demand response," *IEEE Trans. Power Syst.*, vol. 29, no. 5, pp. 2219–2228, Sept. 2014.

[15] R. Poli, J. Kennedy, and T. Blackwell, "Particle swarm optimization: an overview," *Swarm Intell.*, vol. 1, no. 1, pp. 33–57, 2007.

[16] A. A. A. Esmin, G. Lambert-Torres, and A. C. Z. de Souza, "A hybrid particle swarm optimization applied to loss power minimization," *IEEE Trans. Power Syst.*, vol. 20, no. 2, pp. 859–866, 2005.

[17] Z. Luo, Z. Hu, Y. Song, Z. Xu, and H. Lu, "Optimal coordination of plug-in electric vehicles in power grids with cost and benefit analysis - part ii: A case study in china," *IEEE Trans. Power Syst.*, vol. 28, no. 4, pp. 3556–3565, Nov. 2013.

[18] Tesla. "tesla model s specifications". Tesla Motor Corp. [Online]. Available: http://www.teslamotors.com/en_EU/models/specs

[19] Z. Xu, Z. Hu, Y. Song, Z. Luo, K. Zhan, and J. Wu, "Coordinated charging strategy for pevs charging stations," in *Proc. Power and Energy Society General Meeting*, July 2012.

Zhiwei Xu(S'09) received the B.S. degree (with distinction) from Tsinghua University, Beijing, China in July 2011.

He is currently a Ph.D. candidate in the Department of Electrical Engineering at Tsinghua University. He works in the Smart Grid Operation and Optimization Laboratory (SGOOL) as a research assistant. Zhiwei's research interests include electric vehicles, demand response and power systems modeling and operations.

Tianhu Deng received the B.S. degree in Industrial Engineering from Tsinghua University, Beijing, China in 2008, and received the Ph.D. degree in Industrial Engineering & Operations Research from University of California, Berkeley in 2013.

He joined the Department of Industrial Engineering at Tsinghua University in 2013 where he is now an associate professor. His major research interests include optimal planning and operation of natural gas transmission pipeline network, optimization and process flexibility design.

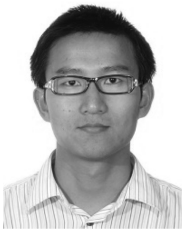

Zechun Hu(M'09) received the B.S. and Ph.D. degrees in electrical engineering from Xi'an Jiao Tong University, Xi'an, China, in 2000 and 2006, respectively.

He was with Shanghai Jiao Tong University, Shanghai, China, and a Research Officer with the University of Bath, Bath, U.K., from 2009 to 2010. He joined the Department of Electrical Engineering, Tsinghua University, Beijing, China, in 2010, where he is currently an Associate Professor. His current research interests include optimal planning and operation of power systems, electric vehicles, and energy storage systems.

Yonghua Song(F'08) received the B.E. degree from the Chengdu University of Science and Technology, Chengdu, China, in 1984, and the Ph.D. degree from the China Electric Power Research Institute, Beijing, China, in 1989, both in electrical engineering.

From 1989 to 1991, he was a Postdoctoral Fellow with Tsinghua University, Beijing. He then held various positions at Bristol University, Bristol, U.K.; Bath University, Bath, U.K.; and John Moores University, Liverpool, U.K., from 1991 to 1996. In 1997, he was a Professor of Power Systems with Brunel University, Uxbridge, U.K., where he has been a Pro-Vice Chancellor for Graduate Studies since 2004. In 2007, he took up a Pro-Vice Chancellorship and Professorship of Electrical Engineering with the University of Liverpool, Liverpool. He was a Professor with the Department of Electrical Engineering, Tsinghua University, where he was an Assistant President and the Deputy Director of the Laboratory of Low-Carbon Energy in 2009. His current research interests include smart grid, electricity economics, and operation and control of power systems.

Prof. Song was a recipient of the D.Sc. Award from Brunel University, in 2002, for his original achievements in power system research. He was elected as the Vice-President of the Chinese Society for Electrical Engineering (CSEE) and appointed as the Chairman of the International Affairs Committee of the CSEE in 2009. In 2004, he was elected as a Fellow of the Royal Academy of Engineering, U.K.

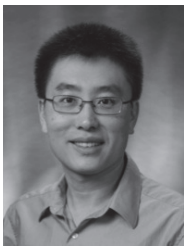

Jianhui Wang(M'07-SM'12) received the Ph.D. degree in electrical engineering from the Illinois Institute of Technology, Chicago, IL, USA, in 2007.

He is currently the Section Lead of Advanced Power Grid Modeling with the Energy Systems Division, Argonne National Laboratory, Argonne, IL. He is also an Affiliate Professor with Auburn University, Auburn, AL, USA, and an Adjunct Professor with the University of Notre Dame, Notre Dame, IN, USA. He has held visiting positions in Europe, Australia, and Hong Kong, including a VELUX Visiting Professorship with the Technical University of Denmark, Lyngby, Denmark.

Dr. Wang was a recipient of the IEEE Power and Energy Society (PES) Power System Operation Committee Prize Paper Award in 2015. He is the Secretary of the IEEE PES Power System Operations Committee. He is an Associate Editor of the *Journal of Energy Engineering* and an Editorial Board Member of *Applied Energy*. He is the Editor-in-Chief of the *IEEE Transactions on Smart Grid* and an IEEE PES Distinguished Lecturer.